scientific reports

Check for updates

OPEN

Bousigonine D from Bousigonia mekongensis inhibits bladder cancer growth and overcomes cisplatin resistance

Kai Shi[1], Xinyuan Li[2], Rui Chen[1], Zhiwei Wang[3], Benkang Shi[1], Ke Wang[4]✉ & Yaofeng Zhu[1]✉

The rising global incidence of bladder cancer and chemotherapy resistance necessitate novel therapies. Plant-derived compounds, owing to their diverse biological activities and favorable safety profiles, are considered promising candidates for cancer treatment. In this study, we investigated Bousigonine D, a monoterpene indole alkaloid isolated from the roots of Bousigonia mekongensis, for its potential as a therapeutic agent for bladder cancer. Our results show that Bousigonine D effectively inhibits cell proliferation and clonogenic formation, and induces cell cycle arrest at the G0/G1 phase in murine and human bladder cancer cells. Furthermore, Bousigonine D significantly promotes apoptosis in these cells, surpassing the apoptosis-inducing efficacy of cisplatin. Mechanistically, Bousigonine D enhances the generation of reactive oxygen species, disrupts calcium homeostasis, and impairs mitochondrial function, leading to cytoskeletal collapse and caspase-dependent apoptotic cell death. In vivo, Bousigonine D effectively suppresses tumor growth in an orthotopic MB49 mouse model, and importantly, it retains strong anti-tumor efficacy in cisplatin-resistant bladder cancer. Notably, Bousigonine D exhibits low toxicity in major organs, similar to cisplatin, underscoring its potential as a safe and effective treatment for bladder cancer. This study highlights the promising role of plant-derived compounds in cancer therapy and supports further development of Bousigonine D as a novel therapeutic option for bladder cancer.

Keywords Bladder cancer, Bousigonine D, Apoptosis, Cisplatin-resistant, Mitochondrial

Bladder cancer is a major public health concern, ranking as the 10th most common cancer globally, with approximately 550,000 new cases and 200,000 deaths annually[1]. The disease predominantly affects older adults, with a higher incidence observed in men[2,3]. Bladder cancer is closely associated with several risk factors, including smoking, occupational exposure to industrial chemicals, chronic urinary tract infections, and genetic predispositions[4,5]. While early-stage bladder cancer is often amenable to treatment with surgery, chemotherapy, and/or radiation, the prognosis for patients with muscle-invasive or metastatic bladder cancer remains poor[6–8]. These advanced stages of disease are characterized by high recurrence rates and limited survival, largely due to the aggressive nature of the cancer and its resistance to conventional therapies.

Cisplatin-based chemotherapy is the standard first-line treatment for muscle-invasive bladder cancer, known for its ability to induce DNA damage and apoptosis in cancer cells[6,9,10]. Despite its initial efficacy, cisplatin resistance is a significant clinical challenge, as it is commonly observed in advanced bladder cancer[11,12]. Cisplatin resistance is multifactorial, involving mechanisms such as reduced drug uptake, enhanced drug efflux, increased DNA repair capacity, evasion of apoptosis, and alterations in the tumor microenvironment[13,14]. As cisplatin resistance develops, treatment options become severely limited, and patient outcomes worsen[15]. Consequently,

[1]Department of Urology, Qilu Hospital, Cheeloo College of Medicine, Shandong University, 107 Cultural West Road, Jinan 250012, Shandong Province, China. [2]Department of Immunology, Shandong Provincial Key Laboratory of Infection and Immunology, School of Basic Medical Sciences, Cheeloo College of Medicine, Shandong University, Jinan 250012, Shandong Province, China. [3]School of Pharmaceutical Sciences & Institute of Materia Medica, Shandong First Medical University & Shandong Academy of Medical Sciences, National Key Laboratory of Advanced Drug Delivery System, Key Laboratory for Biotechnology Drugs of National Health Commission (Shandong Academy of Medical Sciences), Key Lab for Rare & Uncommon Diseases of Shandong Province, Jinan 250117, Shandong, China. [4]Department of Urology, The Affiliated Hospital of Qingdao University, 1677 Wutaishan Road, Qingdao 266001, Shandong Province, China. ✉email: wangke@qdu.edu.cn; Feng2209@163.com

there is an urgent need to identify novel therapeutic agents capable of either circumventing cisplatin resistance or providing an alternative approach to the treatment of bladder cancer.

In recent years, plant-derived compounds have gained considerable attention as potential anticancer agents due to their broad spectrum of biological activities and relatively favorable safety profiles[16,17]. Many plant-based molecules exert their anticancer effects through various mechanisms, including modulation of cell cycle progression, apoptosis induction, oxidative stress regulation, and inhibition of metastasis[18,19]. These compounds offer an advantage over traditional chemotherapy agents due to their lower toxicity, making them especially promising candidates for patients who have developed resistance to standard treatments[20]. Numerous plant-derived alkaloids[21], flavonoids[22], and terpenoids[23] have demonstrated significant anticancer activity across various tumor types, prompting further investigation into their potential for treating bladder cancer.

Bousigonia mekongensis, a plant native to Southeast Asia, has been used in traditional medicine for the treatment of a wide range of ailments, including inflammatory diseases, infections, and metabolic disorders. Although this plant has long been recognized for its therapeutic properties, scientific studies exploring its anticancer potential remain limited. Recent research has isolated several bioactive compounds from Bousigonia mekongensis, including alkaloids and terpenoids, which exhibit notable biological activities such as anti-inflammatory, antimicrobial, and antioxidant effects[24]. However, the potential of Bousigonia mekongensis as a therapeutic agent for bladder cancer has not yet been explored. In our previous studies, we isolated a compound called Bousigonine D from the roots of Bousigonia mekongensis[25]. This monoterpene indole alkaloid demonstrated promising effects in inhibiting mesangial cell proliferation in diabetic nephropathy, where it was shown to effectively suppress glucose-induced mesangial cell proliferation. Despite these encouraging findings, the anticancer properties of Bousigonine D, particularly in bladder cancer, remain unexplored, as well as its underlying molecular mechanisms.

In this study, we investigate the potential of Bounciness D as an anticancer agent for bladder cancer. Specifically, we evaluate its effects on bladder cancer cell proliferation, apoptosis induction, and its ability to overcome splatting resistance. We found that Bounciness D exerts its anticancer effects by modulating critical cellular processes involved in cancer progression, such as oxidative stress, mitochondrial dysfunction, and apoptosis. By investigating the underlying molecular mechanisms of Bounciness D's action, we aim to provide valuable insights into its role in bladder cancer therapy. Ultimately, our findings may contribute to the development of Bounciness D as a prom988ising therapeutic candidate for patients with bladder cancer, particularly those resistant to current chemotherapy regimens.

Methods

Cell culture

Human bladder cancer cell lines T24 and 253 J were obtained from the American Type Culture Collection (ATCC), while the Murine bladder cancer cell line MB49 was purchased from Millilitre. T24 and 253J cells were cultured in RPMI 1640 medium (Gibco, USA), and MB49 cells were cultured in DMEM (Gibco, USA). All media were supplemented with 10% fetal bovine serum (FBS; Gibco, USA) and 1% penicillin–streptomycin (Gibco, USA). Cells were maintained in a humidified incubator at 37 °C with 5% CO_2. For routine subculturing, cells were detached using 0.25% trypsin–EDTA (Gibco, USA) and reseeded at a ratio of 1:3 to 1:5 every 2–3 days. For cryopreservation, cells were resuspended in a freezing medium (90% FBS and 10% DMSO) and stored in liquid nitrogen. All experiments were conducted with mycoplasma-free cells in their exponential growth phase.

Cell viability assay

The SRB assay was used to measure cell viability. Cells were seeded in 96-well plates at a density of 5,000 cells per well, treated with varying concentrations of Bousigonine D or cisplatin for specified durations, and then fixed with 10% trichloroacetic acid (TCA) for 1 h at 4 °C. Fixed cells were washed with distilled water, stained with SRB solution for 30 min, and washed to remove excess dye. The bound dye was solubilized with 10 mM Tris base, and absorbance was measured at 560 nm using a microplate reader. Additionally, crystal violet staining was performed. After treatment, cells were fixed with 4% paraformaldehyde, stained with 0.05% crystal violet for 20 min, and washed with distilled water. Images of stained cells were captured using a microscope equipped with a digital camera.

Colony formation assay

Cells were seeded at a low density (1000 cells/well) in cell dishes and cultured in complete medium for 14 days to allow for colony formation. The medium was replaced every three days. At the endpoint, colonies were fixed with 4% paraformaldehyde for 15 min and stained with 0.05% crystal violet for 15 min. Excess stain was washed off with tap water. Colonies were measured using ImageJ software to quantify clonogenic survival.

Wound healing assay

To evaluate cell migration, a wound healing assay was performed. Cells were seeded in 6-well plates and grown to near confluence. A sterile pipette tip was used to create a straight scratch in the monolayer. Detached cells were removed by washing with PBS, and fresh medium was added. Images of the wound area were captured at 0, 24, and 48 h using a microscope. The wound width at each time point was measured, and the speed of wound closure was calculated to assess migration capacity.

Transwell invasion assay

Cell invasion was assessed using 24-well Transwell plates with 8-μm pore inserts. Cells (5×10^4) in serum-free medium were seeded into the upper chamber, while the lower chamber contained complete medium with 10%

FBS as a chemoattractant. After 24 h of incubation at 37 °C, non-migrated cells were removed, and migrated cells on the lower membrane were fixed with 4% paraformaldehyde, stained with 0.1% crystal violet, and imaged.

Reactive oxygen species (ROS) assay

Intracellular ROS levels were measured using a Reactive Oxygen Species Assay Kit (Beyotime, Shanghai, China). Cells were treated with Bousigonine D or cisplatin, washed with PBS, and incubated with DCFH-DA (10 μM) at 37 °C in the dark for 20 min. Excess probe was removed by washing with PBS. The fluorescence intensity of DCF, an indicator of ROS levels, was measured by flow cytometry.

Annexin V-FITC/PI apoptosis assay

Apoptosis was assessed using the FITC Annexin V Apoptosis Detection Kit I (BD Pharmingen). After 48-h treatments with Bousigonine D or cisplatin, cells were washed with PBS and resuspended in 1× binding buffer. Annexin V-FITC (5 μL) and propidium iodide (PI, 5 μL) were added to 100 μL of the cell suspension, followed by incubation in the dark at room temperature for 15 min. Stained cells were analyzed using a flow cytometer to determine the proportion of apoptotic cells.

Cell cycle analysis

For cell cycle distribution analysis, treated cells were collected, washed with PBS, and fixed in 70% ethanol at 4 °C overnight. Fixed cells were washed, resuspended in PBS containing propidium iodide (PI, 50 μg/mL) and RNase A (100 μg/mL), and incubated in the dark at room temperature for 30 min. The samples were analyzed using flow cytometry, and cell cycle distribution was determined using CytExpert software.

Western blot analysis

Protein extracts were prepared by lysing cells in RIPA buffer supplemented with protease and phosphatase inhibitors (Beyotime, Shanghai, China). Protein concentrations were determined using a BCA Protein Assay Kit. Equal amounts of protein were separated by SDS-PAGE and transferred onto PVDF membranes (Millipore, USA). Membranes were blocked with 5% non-fat milk for 1 h, incubated with primary antibodies overnight at 4 °C, and subsequently incubated with HRP-conjugated secondary antibodies for 1 h at room temperature. Blots were developed using an enhanced chemiluminescence (ECL) substrate, and images were captured using a chemiluminescence detection system (Thermo Fisher Scientific, USA).

Histology and H&E staining

Mouse tissues were fixed in 4% paraformaldehyde, dehydrated through a graded ethanol series, cleared with xylene, and embedded in paraffin. Sections (5 μm) were cut, mounted on slides, and stained with hematoxylin and eosin (H&E). After differentiation and bluing, slides were dehydrated, cleared, and mounted. Tissue morphology was examined under a light microscope.

Immunofluorescence

Cells or paraffin-embedded tissue sections were fixed with 4% paraformaldehyde and permeabilized with 0.1% Triton X-100. After blocking with 1% BSA, samples were incubated with primary antibodies overnight at 4 °C. Fluorescently labeled secondary antibodies were applied for 1 h in the dark, and nuclei were stained with DAPI. Images were acquired using a confocal microscope (Andor Dragonfly 200).

Animal studies

Female C57BL/6 mice (6–8 weeks old) were purchased from Vital River Laboratory Animal Technology (Beijing, China) and housed in specific pathogen-free (SPF) conditions. Mice were acclimated for one week before experiments, with free access to food and water. All procedures were approved by the Animal Care and Use Committee of Qilu Hospital, Shandong University, and followed institutional and national guidelines. Mice were anesthetized by inhalation gas with isoflurane and placed on a pre-warmed heating pad to maintain body temperature during surgery. The lower abdominal area was shaved and disinfected with povidone-iodine and 70% ethanol in a sterile surgical field. Using a microsurgical approach under a surgical microscope, a midline lower abdominal incision was made, and the skin and muscle layers were carefully separated layer by layer to expose the bladder. Luci*MB49 cells or cisplatin-resistant Luci*MB49 cells (5×10^5) were injected beneath the urothelium and above the muscle layer of the bladder wall using a syringe to ensure precise tumor cell delivery. To prevent cell leakage, the needle was held in place for a few seconds before careful withdrawal. Following injection, the bladder was repositioned, and the muscle and skin layers were sequentially sutured using absorbable surgical sutures. Postoperative care included monitoring until full recovery from anesthesia, administration of analgesics, and ensuring the mice resumed normal activity. All surgical procedures were performed under strict aseptic conditions to minimize infection risk. Tumor burden was monitored using bioluminescence imaging. Mice were randomly assigned to treatment groups and treated with Bousigonine D or cisplatin. Tumors were collected at the experimental endpoint for analysis. At the endpoint, mice were euthanized using carbon dioxide (CO_2) inhalation, following established ethical guidelines to minimize distress and ensure humane treatment. The ARRIVE guidelines have been followed for conducting and reporting animal experiments.

Imaging procedure

Bioluminescence imaging was performed to monitor tumor progression. Mice were injected intraperitoneally with D-luciferin (150 mg/kg) and imaged 15 min later using the IVIS Lumina system (PerkinElmer, USA). Luminescence signals were quantified using Living Image Software.

Statistical analysis

All data are presented as mean ± standard deviation (s.d.). Statistical significance was determined using one-way or two-way ANOVA, depending on the experiment. Analyses were conducted using GraphPad Prism Software, with $p < 0.05$ considered statistically significant. Significance levels are indicated as *, **, ***, and **** for $p < 0.05$, 0.01, 0.001, and 0.0001, respectively.

Results

Bousigonine D inhibits bladder cancer cell proliferation and induces cell cycle arrest

The chemical structure of Bousigonine D is shown in Fig. 1A. To evaluate its antiproliferative effects, we treated murine MB49 bladder cancer cells and human T24 and 253 J bladder cancer cells with two concentrations of Bousigonine D and assessed cell viability using the SRB assay. Bousigonine D significantly reduced cell

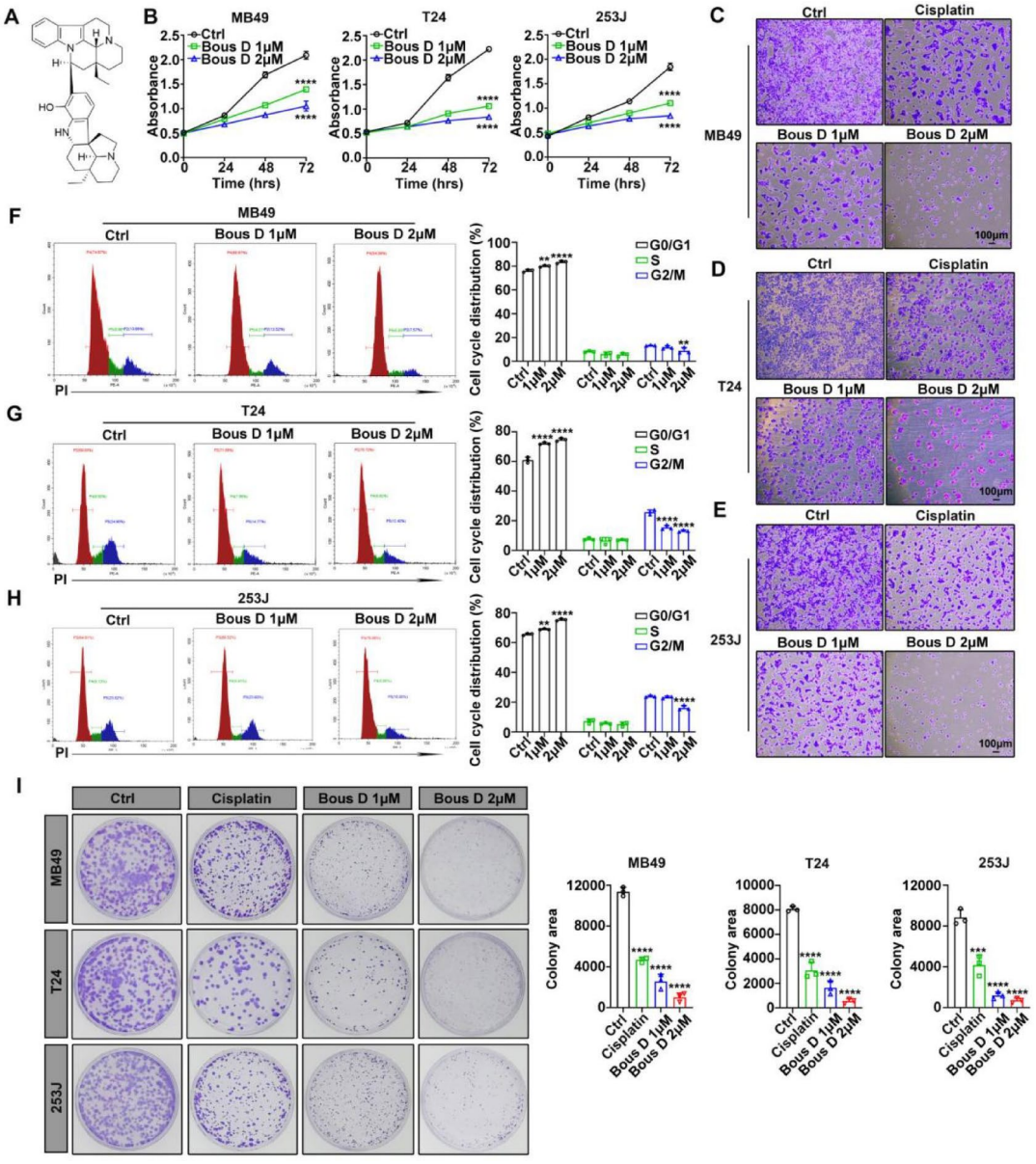

Fig. 1. Bousigonine D inhibits bladder cancer cell proliferation and induces cell cycle arrest in G0/G1. (**A**) Chemical structure of Bousigonine D. (**B**) Cell proliferation in MB49, T24, and 253 J bladder cancer cells was evaluated using the SRB assay following treatment with Bousigonine D. (**C**–**E**) Crystal violet staining of MB49 (**C**), T24 (**D**), and 253 J (**E**) cells treated with cisplatin (2 μM) as a positive control or Bousigonine D (1 μM and 2 μM) for 48 h. (**F**–**H**) Cell cycle distribution was analyzed by flow cytometry in MB49 (**F**), T24 (**G**), and 253 J (**H**) cells after treatment with Bousigonine D, showing G0/G1 arrest. (**I**) Colony formation assays of MB49, T24, and 253 J cells treated with cisplatin (2 μM) or Bousigonine D (1 μM and 2 μM) for 14 days. Data are shown as mean ± s.d. Statistical significance was determined by Two-way ANOVA for (**B**) and One-way ANOVA for (**F-I**). ***$p < 0.001$, ****$p < 0.0001$.

proliferation in a dose-dependent manner across all three cell lines (Fig. 1B). The inhibition of cell proliferation became more pronounced with increasing concentrations of Bousigonine D, demonstrating its strong antiproliferative activity. To further confirm these effects, we performed crystal violet staining to visualize changes in cell density. Consistent with the SRB assay results, treatment with Bousigonine D led to a marked reduction in cell density in MB49, T24, and 253 J cells, with higher concentrations of Bousigonine D showing greater effects compared to cisplatin (Fig. 1C–E). Flow cytometry analysis of the cell cycle revealed that Bousigonine D induced a significant accumulation of cells in the G0/G1 phase in all three cell lines, indicating cell cycle arrest (Fig. 1F–H). This blockade of cell cycle progression is likely a key mechanism underlying the observed antiproliferative effects of Bousigonine D. Additionally, colony formation assays were performed to assess the long-term effects of Bousigonine D on clonogenic survival. Treatment with Bousigonine D significantly inhibited the ability of MB49, T24, and 253 J cells to form colonies over 14 days, further demonstrating its inhibitory effects on cell proliferation (Fig. 1I). These results collectively indicate that Bousigonine D exerts potent antiproliferative effects by inducing G0/G1 cell cycle arrest and suppressing clonogenic survival, with efficacy that is comparable to or exceeds that of cisplatin. This highlights the potential of Bousigonine D as a therapeutic agent for bladder cancer.

Bousigonine D induces apoptosis in bladder cancer cells

To investigate whether the antiproliferative effects of Bousigonine D were mediated by apoptosis, we assessed cell viability and apoptosis using Calcein-AM/PI double staining and flow cytometry. Microscopic observation of MB49, T24, and 253 J cells treated with Bousigonine D showed characteristic features of apoptosis, including cell shrinkage, reduced cell density, and morphological changes (Fig. 2A). Calcein-AM/PI double staining is based on the principle that Calcein-AM stains live cells by entering their cytoplasm, where it is hydrolyzed to a fluorescent product, whereas PI is excluded from live cells but can penetrate the membrane of dead cells, staining their nuclei. Calcein-AM/PI staining confirmed a significant increase in dead cells in Bousigonine D-treated groups compared to cisplatin (Fig. 2B). Flow cytometry analysis using Annexin V/PI double staining demonstrated a marked increase in the proportion of apoptotic cells following treatment with Bousigonine D. The percentage of apoptotic cells in MB49, T24, and 253 J cells was significantly higher in Bousigonine D-treated groups compared to cisplatin-treated controls, with a dose-dependent effect observed (Fig. 2C–E). These results suggest that Bousigonine D not only inhibits cell proliferation but also effectively induces apoptosis in bladder cancer cells. Moreover, Bousigonine D demonstrated superior apoptotic induction compared to cisplatin, highlighting its potential as an alternative therapeutic agent. Collectively, these findings establish apoptosis as a major mechanism underlying the antiproliferative effects of Bousigonine D in bladder cancer cells.

Bousigonine D suppresses bladder cancer cell migration and invasion

The effects of Bousigonine D on bladder cancer cell migration and invasion were assessed using wound healing and transwell invasion assays. In wound healing assays, MB49, T24, and 253 J cells treated with Bousigonine D exhibited significantly reduced wound closure rates at 24 and 48 h compared to cisplatin-treated and control groups, suggesting inhibition of cell migration (Fig. 3A–C). To further evaluate the invasive capacity of bladder cancer cells, transwell invasion assays were performed. Bousigonine D treatment resulted in a significant reduction in the number of invasive cells in all three cell lines, with stronger effects observed at higher concentrations (Fig. 3D–F). These results indicate that Bousigonine D effectively inhibits the invasive potential of bladder cancer cells. Phalloidin staining of the actin cytoskeleton revealed that Bousigonine D disrupted the organization of actin filaments in MB49, T24, and 253 J cells (Fig. 3G–I). This disruption of cytoskeletal integrity may contribute to the reduced migratory and invasive abilities observed in Bousigonine D-treated cells. Together, these findings demonstrate that Bousigonine D suppresses bladder cancer cell migration and invasion, potentially through its effects on cytoskeletal organization.

Bousigonine D induces mitochondrial dysfunction and oxidative stress-mediated apoptosis

To elucidate the mechanisms by which Bousigonine D induces apoptosis in bladder cancer cells, we investigated its effects on ROS production, mitochondrial function, and apoptosis-related pathways. Flow cytometry analysis revealed a significant increase in ROS levels in MB49, T24, and 253 J cells treated with Bousigonine D at concentrations of 1 μM and 2 μM for 24 h, compared to untreated controls and cisplatin-treated cells (Fig. 4A). This elevation in ROS suggests that oxidative stress plays a critical role in the apoptotic effects of Bousigonine D. Elevated calcium levels are known to disrupt mitochondrial homeostasis, promoting mitochondrial dysfunction and triggering apoptosis. Fluo-4 AM staining, which uses the fluorescent probe Fluo-4 AM to detect changes in intracellular calcium levels, revealed significant alterations in calcium levels in Bousigonine D-treated cells, consistent with the induction of apoptosis through calcium dysregulation (Fig. 4B). To further investigate the impact of Bousigonine D on mitochondria, we analyzed mitochondrial morphology and membrane potential. The TOM20 staining technique relies on the mitochondrial outer membrane protein TOM20, and its altered expression indicates changes in mitochondrial morphology. Immunofluorescence staining of TOM20 revealed significant alterations in mitochondrial structure and distribution in cells treated with Bousigonine D, indicative of mitochondrial damage (Fig. 4C). Additionally, JC-1 staining, which is based on the mitochondrial membrane potential ($\Delta\Psi m$)-dependent uptake of the JC-1 dye, showed a substantial loss of mitochondrial membrane potential in Bousigonine D-treated cells, further confirming mitochondrial dysfunction (Fig. 4D). To confirm the activation of apoptotic pathways, we measured cleaved caspase-3 levels using flow cytometry. Bousigonine D treatment significantly upregulated cleaved caspase-3 expression in a dose-dependent manner in bladder cancer cells, compared to cisplatin-treated and untreated controls (Fig. 4E). This finding highlights the activation of caspase-dependent apoptotic pathways, further supporting the pro-apoptotic effects of Bousigonine D. TUNEL assays were employed to evaluate apoptotic DNA fragmentation, a hallmark of apoptosis. The TUNEL assay labels DNA strand breaks, enabling the detection of apoptotic cells. Flow cytometry analysis demonstrated

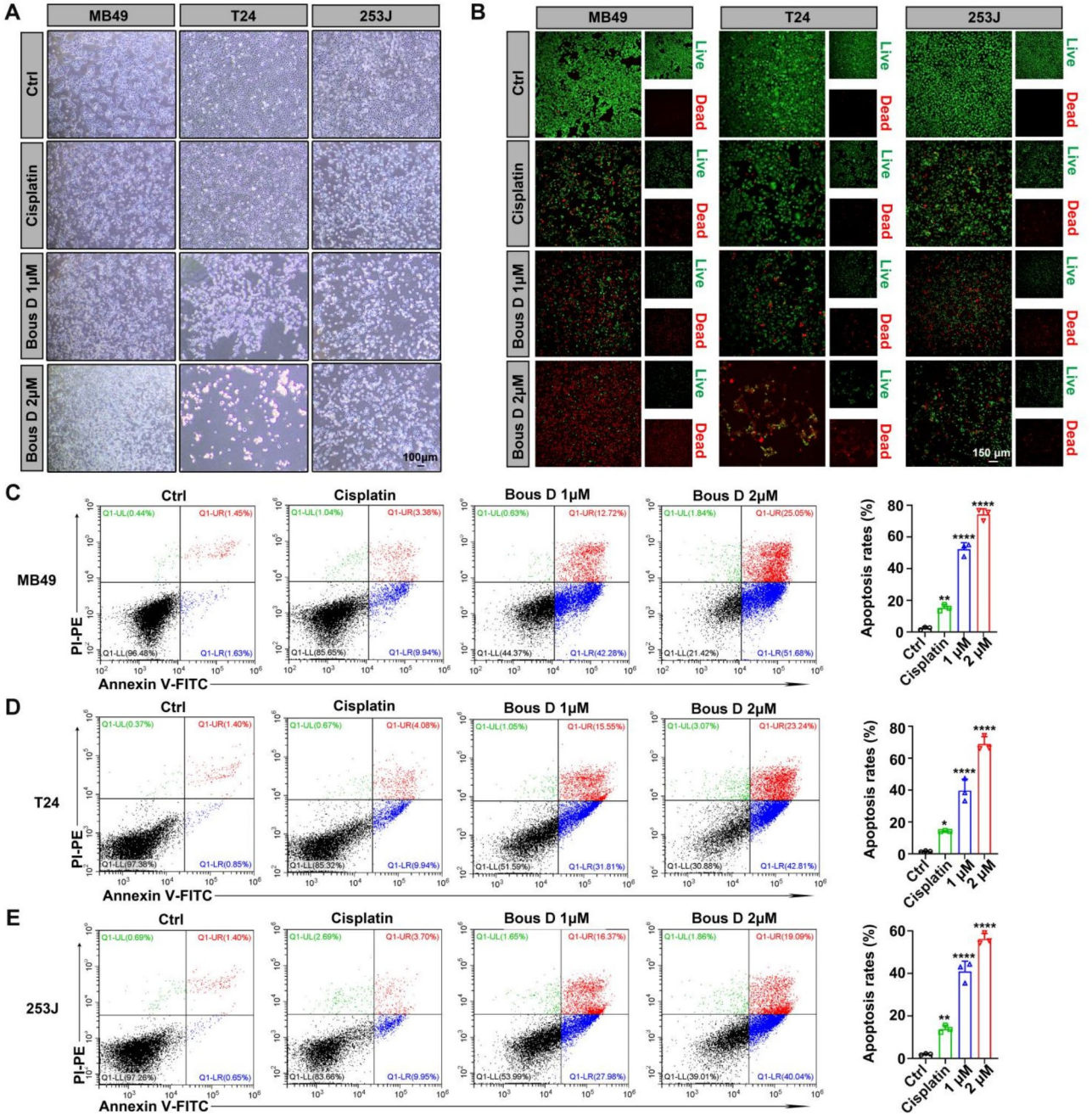

Fig. 2. Bousigonine D induces apoptosis in bladder cancer cells. (**A**) Microscopic examination of cell density and morphology in MB49, T24, and 253 J cells following treatment with cisplatin (2 μM) or Bousigonine D (1 μM and 2 μM) for 48 h. (**B**) Cell viability analysis using the Calcein-AM/PI double staining method to assess live and dead cells in MB49, T24, and 253 J cells treated with cisplatin (2 μM) or Bousigonine D (1 μM and 2 μM). (**C**–**E**) Apoptosis levels in MB49 (**C**), T24 (**D**), and 253 J (**E**) cells were quantified using flow cytometry with Annexin V/PI double staining after treatment with cisplatin (2 μM) or Bousigonine D (1 μM and 2 μM) for 48 h. Data are presented as mean ± s.d. Statistical significance was determined using One-way ANOVA. $^{*}p < 0.05$, $^{**}p < 0.01$, $^{***}p < 0.001$.

a significant increase in TUNEL-positive cells following Bousigonine D treatment, highlighting its ability to induce apoptosis through mitochondrial pathways (Fig. 4F). Western blot analysis provided further molecular evidence for the involvement of mitochondrial pathways in Bousigonine D-induced apoptosis. Treatment with Bousigonine D resulted in the upregulation of cleaved caspase-3, a key effector of apoptosis, and downregulation of anti-apoptotic proteins Bcl-2, Mcl-1 and p-ERK1/2. Furthermore, Cyclin-D1, a regulator of cell cycle progression, was also reduced, consistent with the G0/G1 cell cycle arrest observed previously (Fig. 4G). Collectively, these findings demonstrate that Bousigonine D induces apoptosis in bladder cancer cells through a mechanism involving oxidative stress, caspase activation, calcium dysregulation, and mitochondrial

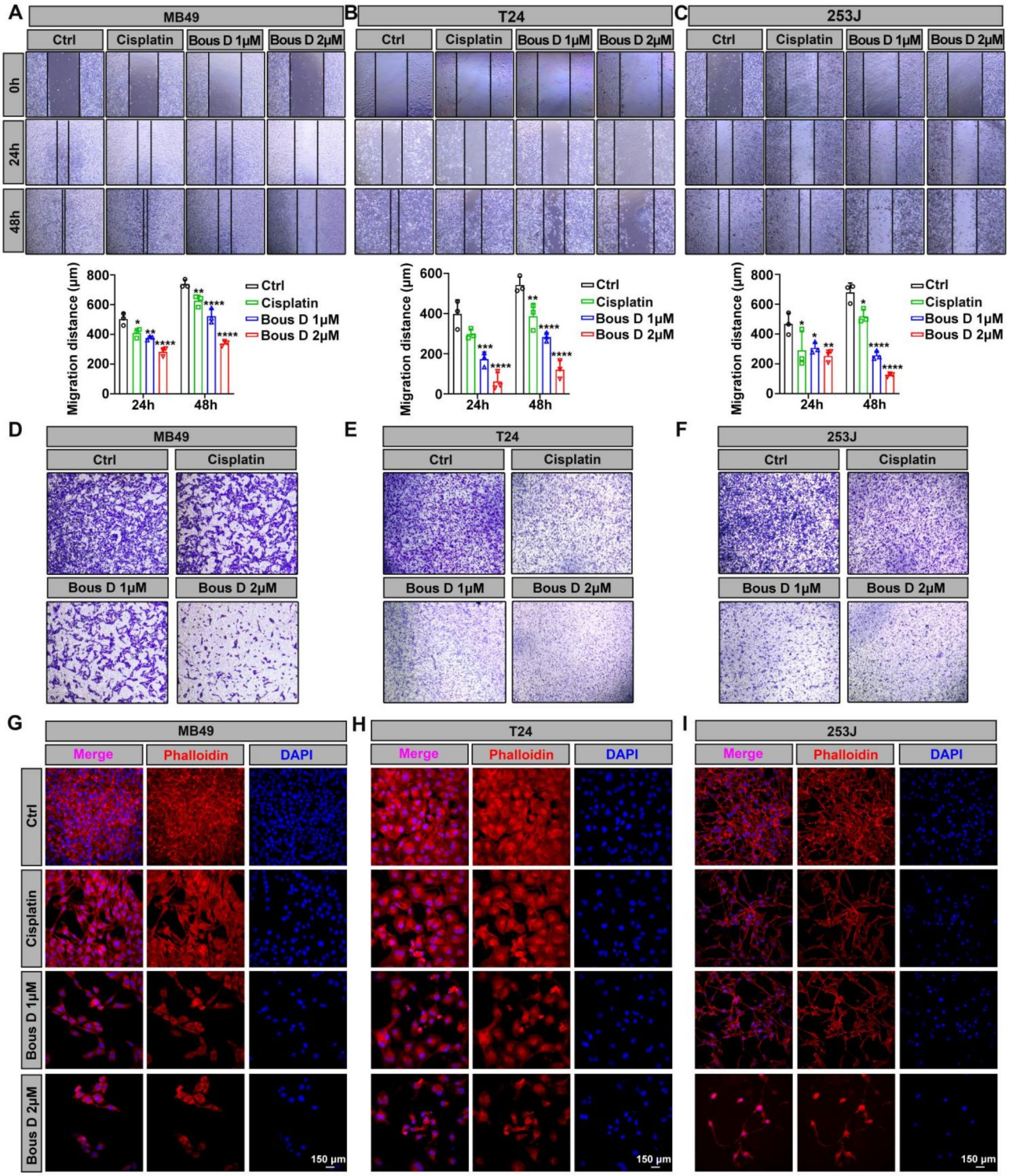

Fig. 3. Bousigonine D inhibits the invasion and migration of bladder cancer cells. (**A**–**C**) Wound healing assays were performed to evaluate the migration ability of MB49 (**A**), T24 (**B**), and 253 J (**C**) cells after treatment with cisplatin (2 μM) or Bousigonine D (1 μM and 2 μM) at 0, 24, and 48 h. (**D**–**F**) Transwell invasion assays were conducted to assess the invasive capacity of MB49 (**D**), T24 (**E**), and 253 J (**F**) cells treated with cisplatin (2 μM) or Bousigonine D (1 μM and 2 μM) for 24 h. (**G**–**I**) Phalloidin immunofluorescence staining was used to visualize the organization of actin filaments in MB49 (**G**), T24 (**H**), and 253 J (**I**) cells following treatment with cisplatin (2 μM) or Bousigonine D (1 μM and 2 μM) for 24 h. Data are presented as mean ± s.d. Statistical significance was determined using One-way ANOVA. $^{*}p < 0.05$, $^{**}p < 0.01$, $^{***}p < 0.001$.

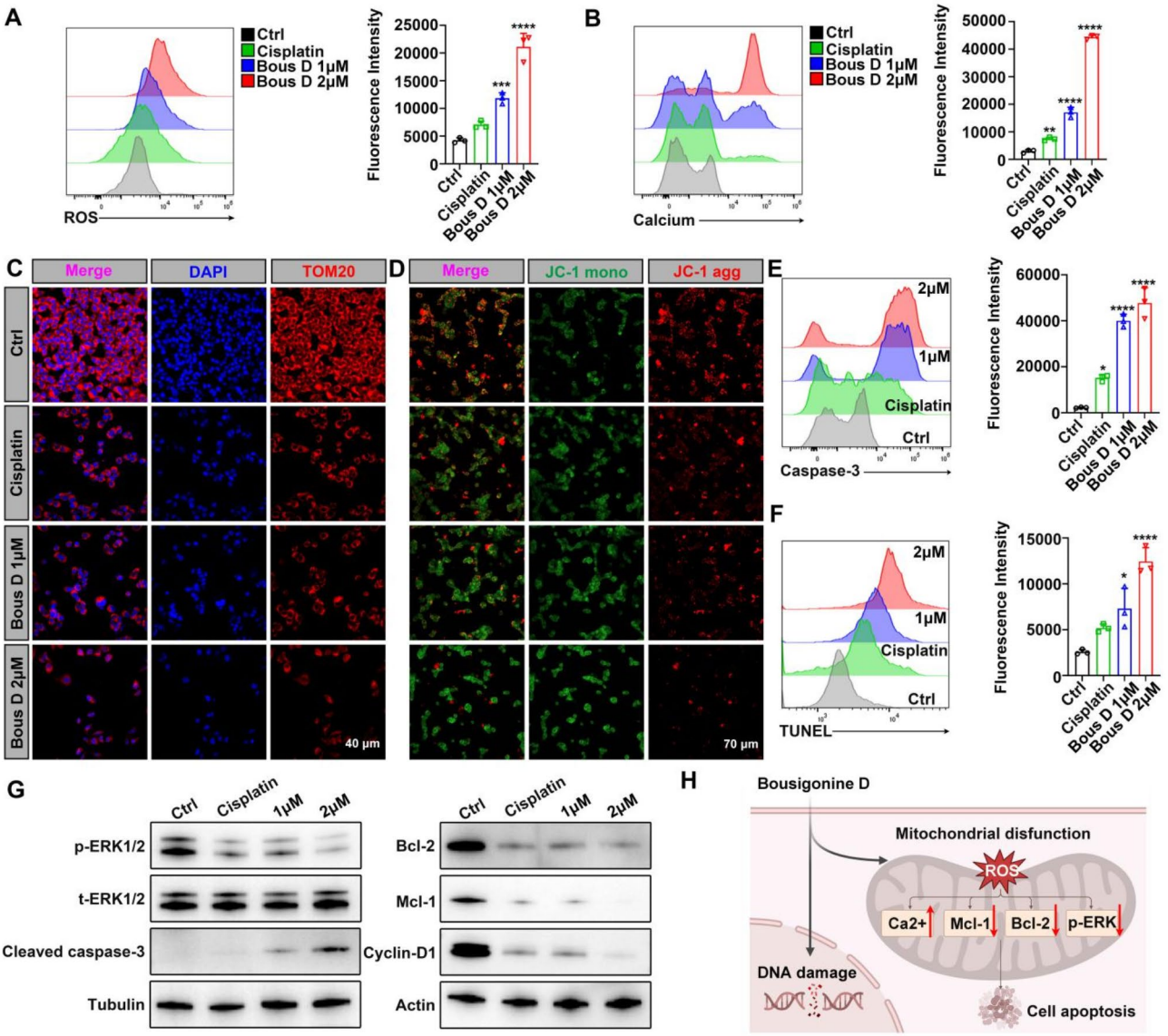

Fig. 4. Bousigonine D induces mitochondrial disruption in bladder cancer cells, leading to apoptosis. (**A**) ROS levels in bladder cancer cells were analyzed by flow cytometry following treatment with cisplatin (2 μM) or Bousigonine D (1 μM and 2 μM) for 24 h. (**B**) Intracellular calcium levels were measured using Fluo-4 AM and analyzed by flow cytometry in bladder cancer cells treated with cisplatin (2 μM) or Bousigonine D (1 μM and 2 μM) for 24 h. (**C**) Mitochondrial morphology and distribution were visualized using TOM20 immunofluorescence staining in bladder cancer cells after treatment with cisplatin (2 μM) or Bousigonine D (1 μM and 2 μM). (**D**) Mitochondrial membrane potential was assessed using JC-1 staining and confocal microscopy in bladder cancer cells treated with cisplatin (2 μM) or Bousigonine D (1 μM and 2 μM) for 24 h. (**E**) Cleaved caspase-3 levels were quantified by flow cytometry to assess apoptosis in bladder cancer cells treated with cisplatin (2 μM) or Bousigonine D (1 μM and 2 μM) for 24 h. (**F**) Apoptotic DNA fragmentation was evaluated using TUNEL assays and analyzed by flow cytometry in bladder cancer cells treated with cisplatin (2 μM) or Bousigonine D (1 μM and 2 μM) for 24 h. (**G**) Western blot analysis of mitochondrial apoptosis-related proteins, including p-ERK1/2, cleaved caspase-3, Bcl-2, Mcl-1, and Cyclin-D1, in bladder cancer cells treated with cisplatin (2 μM) or Bousigonine D (1 μM and 2 μM). (**H**) Schematic illustration of the mechanism of Bousigonine D in bladder cancer cells. Data are presented as mean ± s.d. Statistical significance was determined using One-way ANOVA. $^{*}p < 0.05$, $^{**}p < 0.01$, $^{***}p < 0.001$.

dysfunction. The disruption of mitochondrial membrane potential, altered mitochondrial morphology, and activation of apoptotic pathways underscore the central role of mitochondria in mediating the pro-apoptotic effects of Bousigonine D (Fig. 4H). These results strongly support the therapeutic potential of Bousigonine D as a novel agent targeting mitochondrial dysfunction in bladder cancer therapy.

Bousigonine D suppresses tumor growth in an orthotopic mouse model of bladder cancer

To investigate the therapeutic potential of Bousigonine D in vivo, an orthotopic Luci$^+$ MB49 bladder cancer mouse model was established. The experimental design for treatment with cisplatin and Bousigonine D is illustrated in Fig. 5A. Tumor progression was monitored using bioluminescence imaging over 20 days. Bousigonine D treatment significantly reduced tumor burden in comparison to cisplatin treated and control groups, with noticeable effects as early as day 10 and persisting through day 20 (Fig. 5B, C). These results indicate that Bousigonine D exhibits robust antitumor activity in vivo. Macroscopic examination of excised bladder tumors further confirmed the antitumor effects of Bousigonine D. Tumors from Bousigonine D-treated mice were significantly smaller in size and weight compared to those from cisplatin treated and control groups, highlighting its superior efficacy (Fig. 5D). To understand the cellular effects of Bousigonine D in the tumor microenvironment, immunofluorescence analysis was performed on tumor sections. Ki67 staining revealed a significant reduction in proliferative activity in tumors treated with Bousigonine D, as evidenced by decreased Ki67 expression (Fig. 5E). Furthermore, TUNEL staining showed a marked increase in apoptotic cells in the Bousigonine D-treated group, indicating that its antitumor effects are mediated by enhanced apoptosis (Fig. 5F). Overall, these results demonstrate that Bousigonine D effectively suppresses bladder cancer growth in an orthotopic mouse model by reducing tumor proliferation and promoting apoptosis. Its efficacy in vivo underscores its potential as a promising therapeutic agent for bladder cancer.

Bousigonine D retains efficacy in cisplatin-resistant bladder cancer models

To evaluate whether Bousigonine D can overcome cisplatin resistance, a cisplatin-resistant Luci$^+$ MB49 bladder cancer mouse model was established. The experimental design is shown in Fig. 6A. Tumor progression was monitored using bioluminescence imaging. Mice treated with Bousigonine D exhibited a significant reduction in tumor burden compared to the cisplatin-treated group, with effects becoming evident as early as day 10 and persisting through day 20 (Fig. 6B, C). Quantitative analysis of bioluminescence intensity confirmed the robust inhibitory effects of Bousigonine D, even in cisplatin-resistant tumors, demonstrating its ability to effectively suppress tumor growth in this challenging context. Macroscopic examination of excised tumors further supported the efficacy of Bousigonine D. Tumors from the Bousigonine D-treated group were significantly smaller in size and weight compared to those from the cisplatin-treated group, highlighting its superior antitumor activity

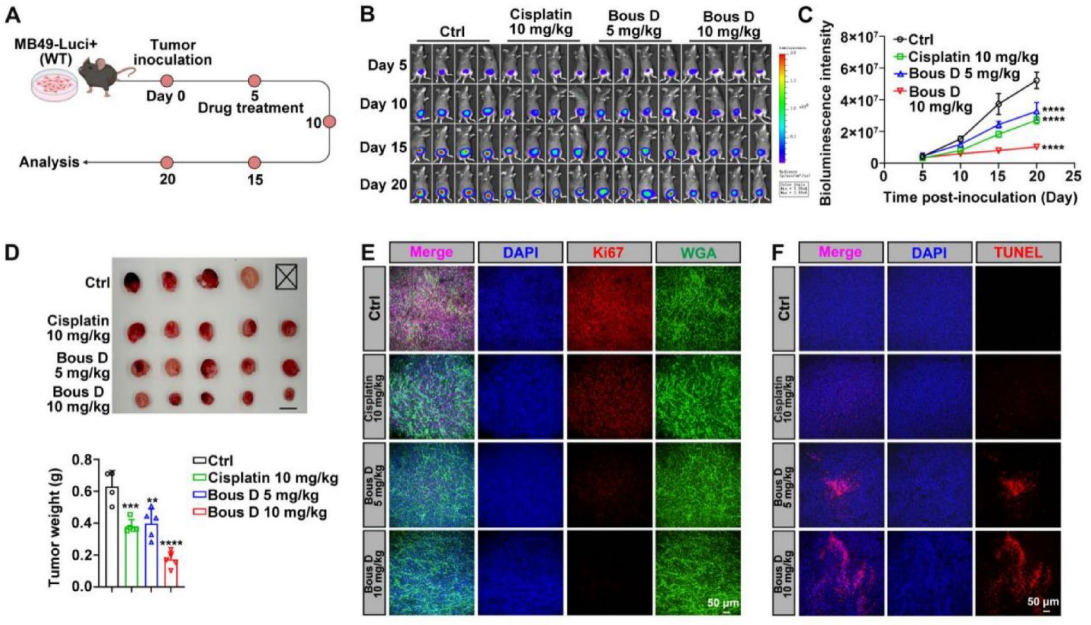

Fig. 5. Bousigonine D inhibits bladder cancer growth in an orthotopic mouse model. (**A**) Schematic representation of the experimental design for the treatment of Luci + MB49 tumor-bearing C57BL/6 mice with cisplatin and Bousigonine D. (**B**) Bioluminescence images of Luci + MB49 tumor-bearing C57BL/6 mice on days 5, 10, 15, and 20 post-treatment with cisplatin or Bousigonine D. (**C**) Quantitative analysis of bioluminescence intensity in Luci + MB49 tumor-bearing C57BL/6 mice at days 5, 10, 15, and 20 following treatment with cisplatin or Bousigonine D. (**D**) Representative macroscopic images of excised bladder tumors from Luci + MB49 tumor-bearing C57BL/6 mice treated with cisplatin or Bousigonine D. Scale bars represent 1 cm (up). Tumor weight measurements of excised Luci + MB49 tumors from C57BL/6 mice following treatment with cisplatin or Bousigonine D (low). (**E**) Immunofluorescence staining for Ki67 (red, proliferation marker), WGA (green, cell membrane marker), and DAPI (blue, nuclear stain) in tumor sections from C57BL/6 mice. Scale bars: 50 μm. (**F**) Immunofluorescence staining for TUNEL (red, apoptotic marker) and DAPI (blue, nuclear stain) in tumor sections from C57BL/6 mice. Scale bars: 50 μm. Data are presented as mean ± s.d. Statistical significance was determined using One-way ANOVA. $^*p < 0.05$, $^{**}p < 0.01$, $^{***}p < 0.001$.

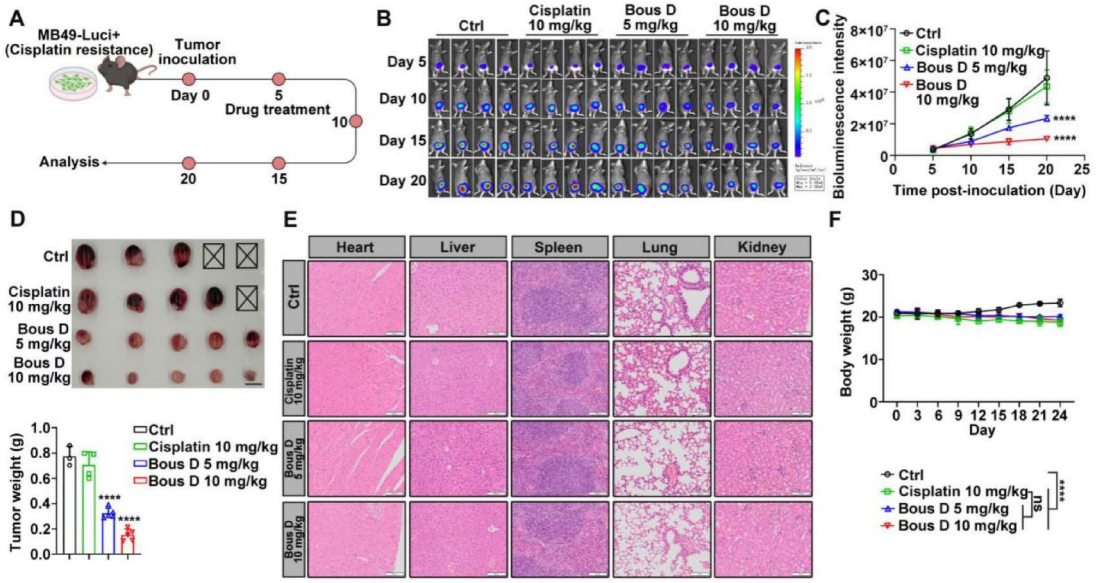

Fig. 6. Bousigonine D exhibits inhibitory effects in a cisplatin-resistant mouse model of bladder cancer. (**A**) Schematic representation of the experimental design for the cisplatin-resistant Luci + MB49 tumor-bearing C57BL/6 mouse model. (**B**) Bioluminescence images of cisplatin-resistant Luci + MB49 tumor-bearing C57BL/6 mice at days 5, 10, 15, and 20 following treatment with cisplatin or Bousigonine D. (**C**) Quantitative analysis of bioluminescence intensity in cisplatin-resistant Luci + MB49 tumor-bearing C57BL/6 mice at days 5, 10, 15, and 20 after treatment with cisplatin or Bousigonine D. (**D**) Macroscopic images of excised bladder tumors from cisplatin-resistant Luci + MB49 tumor-bearing C57BL/6 mice treated with cisplatin or Bousigonine D. Scale bars represent 1 cm (up). Tumor weight measurements of excised bladder tumors from cisplatin-resistant Luci + MB49 tumor-bearing C57BL/6 mice treated with cisplatin or Bousigonine D (low). (**E**) Hematoxylin and eosin (H&E) staining of heart, liver, spleen, lung, and kidney tissues from mice treated with cisplatin or Bousigonine D to evaluate potential organ toxicity. (**F**) Body weight monitoring of cisplatin-resistant Luci + MB49 tumor-bearing C57BL/6 mice during treatment with cisplatin or Bousigonine D. Data are presented as mean ± s.d. Statistical significance was determined using One-way ANOVA. ns: no significance, $^{*}p < 0.05$, $^{**}p < 0.01$, $^{***}p < 0.001$.

in cisplatin-resistant bladder cancer (Fig. 6D). To assess the safety profile of Bousigonine D, hematoxylin and eosin (H&E) staining was performed on major organs, including the heart, liver, spleen, lung, and kidney. No significant histopathological abnormalities were observed in Bousigonine D-treated mice, suggesting minimal systemic toxicity (Fig. 6E). Furthermore, body weight monitoring revealed a modest reduction in the drug-treated groups (Fig. 6F), with Bousigonine D showing similar effects to cisplatin. This modest weight loss highlights the need for a more comprehensive toxicity evaluation before advancing to clinical trials. Together, these results demonstrate that Bousigonine D not only retains its antitumor efficacy in cisplatin-resistant bladder cancer models but also maintains a low toxicity profile, making it a promising therapeutic candidate for the treatment of cisplatin-resistant bladder cancer.

Discussion

Bladder cancer remains one of the most prevalent malignancies worldwide, and despite the availability of chemotherapy options like cisplatin, the survival rates for advanced or metastatic bladder cancer patients remain dismal[26]. One of the primary challenges in the treatment of BC is the development of resistance to chemotherapy, particularly cisplatin, which has long been the cornerstone of treatment for muscle-invasive bladder cancer[6,7,27]. Cisplatin resistance complicates the clinical management of BC and is associated with poor prognosis and limited therapeutic options[11,13]. As a result, there is an urgent need for novel agents that can either overcome resistance or provide a viable alternative for patients who fail conventional therapies. Plant-derived compounds, which have gained significant attention in recent years, represent a promising avenue for the development of new cancer treatments due to their diverse biological activities and generally favorable safety profiles[17,28].

Numerous plant-derived compounds, including flavonoids, alkaloids, and terpenoids, have shown significant anticancer potential through mechanisms such as apoptosis induction, cell cycle regulation, oxidative stress modulation, and metastasis inhibition[29–31]. These compounds often exhibit lower toxicity compared to conventional chemotherapy agents, making them especially promising for treating chemotherapy-resistant cancers[32]. Alkaloids and terpenoids, in particular, have demonstrated potent anticancer properties by targeting various pathways involved in cancer progression[33,34]. Several studies have highlighted the potential of these plant-derived compounds in bladder cancer, with promising effects observed in preclinical models[35–38]. However, despite the growing body of evidence supporting their anticancer potential, there remains a lack of in-depth studies on their effects on cisplatin-resistant bladder cancer and the mechanisms underlying their

action. Historically, several plant-derived compounds, such as paclitaxel, vincristine, vinblastine, etoposide, and topotecan, have proven their clinical efficacy, further underscoring the vast potential of natural products in cancer treatment[12,39–42]. These compounds have been pivotal in modern cancer therapies, illustrating the considerable therapeutic promise of plant-derived agents in the fight against various malignancies.

In light of these successful examples, the search for novel plant-derived agents with anticancer activity continues to be a highly fruitful area of research. In this context, the present study explores the anticancer potential of Bousigonine D, a monoterpene indole alkaloid isolated from Bousigonia mekongensis[25]. Our results demonstrate that Bousigonine D effectively inhibits bladder cancer cell proliferation, induces apoptosis, and significantly overcomes cisplatin resistance. These findings are consistent with the broader body of research showing that plant-derived compounds can effectively target cisplatin-resistant cancer cells by modulating cellular processes such as oxidative stress, mitochondrial dysfunction, and apoptosis. We acknowledge that the concentration of cisplatin used in our study (2 μM) is relatively mild. Therefore, while Bousigonine D demonstrated superior apoptotic effects compared to cisplatin at the tested concentrations, additional studies using higher cisplatin doses are necessary to fully evaluate its comparative efficacy.

The anticancer activity of Bousigonine D appears to be largely attributed to its ability to induce significant oxidative stress, as evidenced by the increased production of ROS in bladder cancer cells. ROS generation has long been recognized as a key mechanism through which many anticancer agents exert their cytotoxic effects[43]. Elevated ROS levels can damage cellular macromolecules, including lipids, proteins, and DNA, ultimately leading to cell death. This process is especially effective in cancer cells, which often exhibit dysregulated redox balance. In line with previous research, our study suggests that Bousigonine D exploits this vulnerability in bladder cancer cells to promote apoptosis. Additionally, our findings that Bousigonine D disrupts mitochondrial function and alters mitochondrial membrane potential further corroborate its role in inducing apoptosis through the intrinsic pathway. These mechanisms have been well-documented in other plant-derived anticancer agents, highlighting the consistency of Bousigonine D's actions with other natural compounds[44].

Moreover, the ability of Bousigonine D to overcome cisplatin resistance is particularly noteworthy. Cisplatin resistance is a multifactorial phenomenon involving reduced drug uptake, enhanced drug efflux, activation of DNA repair mechanisms, and evasion of apoptosis. Previous studies have identified several compounds, including plant-derived molecules, that can circumvent these resistance mechanisms by targeting alternative cellular pathways[45,46]. For example, natural products like curcumin, resveratrol, and certain flavonoids have been shown to modulate apoptosis-related proteins and enhance the efficacy of cisplatin in resistant cancer cells[47–49]. Bousigonine D shares similar properties, as our results indicate that it can induce apoptosis in cisplatin-resistant bladder cancer cells by activating caspase-dependent pathways and inhibiting anti-apoptotic proteins such as Mcl-1 and Bcl-2. This ability to bypass common mechanisms of cisplatin resistance underscores the therapeutic potential of Bousigonine D for patients with refractory bladder cancer. We recognize that additional experiments are required to draw definitive conclusions regarding the clinical applicability of Bousigonine D in cisplatin-resistant bladder cancer. Future studies should focus on evaluating its effects in well-established cisplatin-resistant cell lines and in vivo models to further validate its therapeutic potential.

Despite the promising results observed in this study, there are several key considerations for future research. While we have demonstrated the efficacy of Bousigonine D in preclinical models, further studies are necessary to better understand its pharmacokinetics and pharmacodynamics. Specifically, the bioavailability and metabolic stability of Bousigonine D need to be thoroughly investigated to optimize its therapeutic application. Additionally, identifying the precise molecular targets of Bousigonine D will provide deeper insights into its mechanisms of action and allow for the development of potential biomarkers to guide patient selection. Future studies utilizing metastatic bladder cancer models will be necessary to further evaluate its potential in inhibiting tumor spread. Lastly, the potential for combination therapies involving Bousigonine D and other chemotherapeutic agents, particularly cisplatin, should be explored to determine if synergistic effects can further enhance therapeutic outcomes.

In conclusion, Bousigonine D represents a promising novel therapeutic agent for bladder cancer, particularly for patients who have developed resistance to cisplatin-based treatments. Through its ability to induce apoptosis, modulate oxidative stress, and overcome cisplatin resistance, Bousigonine D shows considerable potential as a safe and effective treatment for bladder cancer. These findings contribute to the growing body of evidence supporting the development of plant-derived compounds as effective cancer therapies and offer hope for improving the treatment of bladder cancer, especially in cases where conventional chemotherapy options have failed. Future studies will be crucial in advancing Bousigonine D from preclinical models to clinical trials, paving the way for its potential inclusion in bladder cancer treatment regimens. The success of plant-derived compounds like paclitaxel, vincristine, and topotecan in clinical settings further emphasizes the enormous potential for new natural products to play a pivotal role in cancer treatment.

Data availability

The original contributions presented in the study are included in the article, further inquiries can be directed to the corresponding author.

Received: 17 January 2025; Accepted: 1 April 2025
Published online: 09 May 2025

References

1. Sung, H. et al. Global cancer statistics 2020: GLOBOCAN estimates of incidence and mortality worldwide for 36 cancers in 185 countries. *CA Cancer J. Clin.* **71**, 209–249. https://doi.org/10.3322/caac.21660 (2021).

2. Dobruch, J. et al. Gender and bladder cancer: A collaborative review of etiology, biology, and outcomes. *Eur. Urol.* **69**, 300–310. https://doi.org/10.1016/j.eururo.2015.08.037 (2016).
3. Dyrskjøt, L. et al. Bladder cancer. *Nat. Rev. Dis. Primers* **9**, 58. https://doi.org/10.1038/s41572-023-00468-9 (2023).
4. Lenis, A. T., Lec, P. M., Chamie, K. & Mshs, M. D. Bladder cancer: A review. *JAMA* **324**, 1980–1991. https://doi.org/10.1001/jama.2020.17598 (2020).
5. Jubber, I. et al. Epidemiology of bladder cancer in 2023: A systematic review of risk factors. *Eur. Urol.* **84**, 176–190. https://doi.org/10.1016/j.eururo.2023.03.029 (2023).
6. Alfred Witjes, J. et al. European association of urology guidelines on muscle-invasive and metastatic bladder cancer: Summary of the 2023 guidelines. *Eur. Urol.* **85**, 17–31. https://doi.org/10.1016/j.eururo.2023.08.016 (2024).
7. Compérat, E. et al. Current best practice for bladder cancer: A narrative review of diagnostics and treatments. *Lancet* **400**, 1712–1721. https://doi.org/10.1016/s0140-6736(22)01188-6 (2022).
8. Flaig, T. W. et al. NCCN Guidelines® Insights: Bladder Cancer, Version 3.2024. *J. Natl. Compr. Cancer Netw.* **22**, 216–225. https://doi.org/10.6004/jnccn.2024.0024 (2024).
9. Nadal, R., Valderrama, B. P. & Bellmunt, J. Progress in systemic therapy for advanced-stage urothelial carcinoma. *Nat. Rev. Clin. Oncol.* **21**, 8–27. https://doi.org/10.1038/s41571-023-00826-2 (2024).
10. Funt, S. A. & Rosenberg, J. E. Systemic, perioperative management of muscle-invasive bladder cancer and future horizons. *Nat. Rev. Clin. Oncol.* **14**, 221–234. https://doi.org/10.1038/nrclinonc.2016.188 (2017).
11. Alifrangis, C., McGovern, U., Freeman, A., Powles, T. & Linch, M. Molecular and histopathology directed therapy for advanced bladder cancer. *Nat. Rev. Urol.* **16**, 465–483. https://doi.org/10.1038/s41585-019-0208-0 (2019).
12. Liu, D. et al. Mutational patterns in chemotherapy resistant muscle-invasive bladder cancer. *Nat. Commun.* **8**, 2193. https://doi.org/10.1038/s41467-017-02320-7 (2017).
13. Li, F. et al. Regulation of cisplatin resistance in bladder cancer by epigenetic mechanisms. *Drug Resist. Updates* **68**, 100938. https://doi.org/10.1016/j.drup.2023.100938 (2023).
14. Shi, Z. D. et al. Targeting HNRNPU to overcome cisplatin resistance in bladder cancer. *Mol. Cancer* **21**, 37. https://doi.org/10.1186/s12943-022-01517-9 (2022).
15. Roviello, G., Santoni, M., Sonpavde, G. P. & Catalano, M. The evolving treatment landscape of metastatic urothelial cancer. *Nat. Rev. Urol.* **21**, 580–592. https://doi.org/10.1038/s41585-024-00872-0 (2024).
16. Newman, D. J. & Cragg, G. M. Natural products as sources of new drugs over the nearly four decades from 01/1981 to 09/2019. *J. Nat. Prod.* **83**, 770–803. https://doi.org/10.1021/acs.jnatprod.9b01285 (2020).
17. Faguet, G. From periwinkle to an enduring anticancer drug. *Lancet Oncol.* **22**, 308. https://doi.org/10.1016/s1470-2045(20)30588-x (2021).
18. Atanasov, A. G., Zotchev, S. B., Dirsch, V. M. & Supuran, C. T. Natural products in drug discovery: Advances and opportunities. *Nat. Rev. Drug Discov.* **20**, 200–216. https://doi.org/10.1038/s41573-020-00114-z (2021).
19. Tewari, D., Patni, P., Bishayee, A., Sah, A. N. & Bishayee, A. Natural products targeting the PI3K-Akt-mTOR signaling pathway in cancer: A novel therapeutic strategy. *Semin. Cancer Biol.* **80**, 1–17. https://doi.org/10.1016/j.semcancer.2019.12.008 (2022).
20. Wang, Y. et al. New drug discovery and development from natural products: Advances and strategies. *Pharmacol. Ther.* **264**, 108752. https://doi.org/10.1016/j.pharmthera.2024.108752 (2024).
21. Qin, R. et al. Naturally derived indole alkaloids targeting regulated cell death (RCD) for cancer therapy: From molecular mechanisms to potential therapeutic targets. *J. Hematol. Oncol.* **15**, 133. https://doi.org/10.1186/s13045-022-01350-z (2022).
22. Bondonno, N. P. et al. Flavonoid intake is associated with lower mortality in the Danish Diet Cancer and Health Cohort. *Nat. Commun.* **10**, 3651. https://doi.org/10.1038/s41467-019-11622-x (2019).
23. Kuang, Y., Li, B., Wang, Z., Qiao, X. & Ye, M. Terpenoids from the medicinal mushroom Antrodia camphorata: Chemistry and medicinal potential. *Nat Prod Rep* **38**, 83–102. https://doi.org/10.1039/d0np00023j (2021).
24. Zhang, Y. et al. Antiproliferative aspidosperma-type monoterpenoid indole alkaloids from Bousigonia mekongensis inhibit tubulin polymerization. *Molecules* **24**, 1256. https://doi.org/10.3390/molecules24071256 (2019).
25. Wang, Z.-W., Wang, Y.-L., Zhang, J.-P., Wei, Q.-H. & Wang, X.-J. Monoterpene indole alkaloids from the roots of Bousigonia mekongensis and their anti-diabetic nephropathy activity. *Fitoterapia* **153**, 104964. https://doi.org/10.1016/j.fitote.2021.104964 (2021).
26. Moschini, M. et al. Bladder cancer: ESMO clinical practice guideline for diagnosis, treatment and follow-up. *Ann. Oncol.* **33**, 561. https://doi.org/10.1016/j.annonc.2022.01.075 (2022).
27. Lopez-Beltran, A., Cookson, M. S., Guercio, B. J. & Cheng, L. Advances in diagnosis and treatment of bladder cancer. *BMJ* **384**, e076743. https://doi.org/10.1136/bmj-2023-076743 (2024).
28. Bishayee, A. & Sethi, G. Bioactive natural products in cancer prevention and therapy: Progress and promise. *Semin. Cancer Biol.* **40–41**, 1–3. https://doi.org/10.1016/j.semcancer.2016.08.006 (2016).
29. Birt, D. F., Hendrich, S. & Wang, W. Dietary agents in cancer prevention: flavonoids and isoflavonoids. *Pharmacol. Ther.* **90**, 157–177. https://doi.org/10.1016/s0163-7258(01)00137-1 (2001).
30. Selvakumar, P. et al. Flavonoids and other polyphenols act as epigenetic modifiers in breast cancer. *Nutrients* **12**, 761. https://doi.org/10.3390/nu12030761 (2020).
31. Sitarek, P. et al. Flavonoids and their derivatives as DNA topoisomerase inhibitors with anti-cancer activity in various cell models: Exploring a novel mode of action. *Pharmacol Res* **209**, 107457. https://doi.org/10.1016/j.phrs.2024.107457 (2024).
32. Liang, Y. et al. Nanoplatform-based natural products co-delivery system to surmount cancer multidrug-resistant. *J. Control Release* **336**, 396–409. https://doi.org/10.1016/j.jconrel.2021.06.034 (2021).
33. Gu, C. et al. Identification of berberine as a novel drug for the treatment of multiple myeloma via targeting UHRF1. *BMC Biol.* **18**, 33. https://doi.org/10.1186/s12915-020-00766-8 (2020).
34. Schneider-Stock, R., Ghantous, A., Bajbouj, K., Saikali, M. & Darwiche, N. Epigenetic mechanisms of plant-derived anticancer drugs. *Front Biosci. (Landmark Ed.)* **17**, 129–173. https://doi.org/10.2741/3919 (2012).
35. Abbaoui, B., Lucas, C. R., Riedl, K. M., Clinton, S. K. & Mortazavi, A. Cruciferous vegetables, isothiocyanates, and bladder cancer prevention. *Mol. Nutr. Food Res.* **62**, e1800079. https://doi.org/10.1002/mnfr.201800079 (2018).
36. Kwan, M. L. et al. The influence of dietary isothiocyanates on the effectiveness of mitomycin C and bacillus Calmette-Guérin in treating nonmuscle-invasive bladder cancer. *J. Urol.* **212**, 420–430. https://doi.org/10.1097/ju.0000000000004070 (2024).
37. Sáez, V. et al. Oligostilbenoids in Vitis vinifera L. Pinot Noir grape cane extract: Isolation, characterization, in vitro antioxidant capacity and anti-proliferative effect on cancer cells. *Food Chem.* **265**, 101–110. https://doi.org/10.1016/j.foodchem.2018.05.050 (2018).
38. Xie, H. et al. Plant-derived sulforaphane suppresses growth and proliferation of drug-sensitive and drug-resistant bladder cancer cell lines in vitro. *Cancers (Basel)* **14**, 4682. https://doi.org/10.3390/cancers14194682 (2022).
39. Baize, N. et al. Carboplatin plus etoposide versus topotecan as second-line treatment for patients with sensitive relapsed small-cell lung cancer: an open-label, multicentre, randomised, phase 3 trial. *Lancet Oncol.* **21**, 1224–1233. https://doi.org/10.1016/s1470-2045(20)30461-7 (2020).
40. Choi, Y. et al. Novel insights into paclitaxel's role on tumor-associated macrophages in enhancing PD-1 blockade in breast cancer treatment. *J. Immunother. Cancer* https://doi.org/10.1136/jitc-2024-008864 (2024).

41. Pfister, C. et al. Perioperative dose-dense methotrexate, vinblastine, doxorubicin, and cisplatin in muscle-invasive bladder cancer (VESPER): survival endpoints at 5 years in an open-label, randomised, phase 3 study. *Lancet Oncol.* **25**, 255–264. https://doi.org/10.1016/s1470-2045(23)00587-9 (2024).
42. Defachelles, A. S. et al. Randomized phase II trial of vincristine-irinotecan with or without temozolomide, in children and adults with relapsed or refractory rhabdomyosarcoma: A European paediatric soft tissue sarcoma study group and innovative therapies for children with cancer trial. *J. Clin. Oncol.* **39**, 2979–2990. https://doi.org/10.1200/jco.21.00124 (2021).
43. Glorieux, C., Liu, S., Trachootham, D. & Huang, P. Targeting ROS in cancer: Rationale and strategies. *Nat. Rev. Drug Discov.* **23**, 583–606. https://doi.org/10.1038/s41573-024-00979-4 (2024).
44. Fontana, F. et al. Unraveling the molecular mechanisms and the potential chemopreventive/therapeutic properties of natural compounds in melanoma. *Semin. Cancer Biol.* **59**, 266–282. https://doi.org/10.1016/j.semcancer.2019.06.011 (2019).
45. Efferth, T. et al. Collateral sensitivity of natural products in drug-resistant cancer cells. *Biotechnol. Adv.* **38**, 107342. https://doi.org/10.1016/j.biotechadv.2019.01.009 (2020).
46. AlQathama, A. & Prieto, J. M. Natural products with therapeutic potential in melanoma metastasis. *Nat. Prod. Rep.* **32**, 1170–1182. https://doi.org/10.1039/c4np00130c (2015).
47. Patra, S. et al. Chemotherapeutic efficacy of curcumin and resveratrol against cancer: Chemoprevention, chemoprotection, drug synergism and clinical pharmacokinetics. *Semin. Cancer Biol.* **73**, 310–320. https://doi.org/10.1016/j.semcancer.2020.10.010 (2021).
48. Weng, W. & Goel, A. Curcumin and colorectal cancer: An update and current perspective on this natural medicine. *Semin. Cancer Biol.* **80**, 73–86. https://doi.org/10.1016/j.semcancer.2020.02.011 (2022).
49. Cai, J. et al. Flavonoids and gastric cancer therapy: From signaling pathway to therapeutic significance. *Drug Des. Dev. Ther.* **18**, 3233–3253. https://doi.org/10.2147/dddt.S466470 (2024).

Acknowledgements

The author would like to thank M.L.W., and L.M.W. for their technical support from the Advanced Medical Research Institute/Translational Medicine Core Facility of Shandong University. All schematic figures were created with BioRender.com.

Author contributions

KS wrote the main manuscript text. KS, XL, and RC provided methodology, analyzed data and prepared figure 1–6. ZW provided compounds required for the research. BS supervised the study and manuscript writing process. KW conceptualized and supervised the study. YZ provided funding acquisition and project administration, conceptualized and supervised the study. All authors reviewed the manuscript.

Funding

The authors declare that financial support was received for the research, authorship, and/or publication of this article. This research was funded by the Natural Science Foundation of Shandong Province (ZR2021MH318 to YZ and ZR2024MH024 to KW).

Declarations

Competing interests

The authors declare no competing interests.

Additional information

Supplementary Information The online version contains supplementary material available at https://doi.org/10.1038/s41598-025-96892-w.

Correspondence and requests for materials should be addressed to K.W. or Y.Z.